

Coincidence analysis to search for inspiraling compact binaries

Hiroataka Takahashi^{†‡§}, Hideyuki Tagoshi[†] the TAMA
Collaboration and the LISM Collaboration

[†] Department of Earth and Space Science, Graduate School of Science, Osaka
University, Toyonaka, Osaka 560-0043, Japan

[‡] Graduate School of Science and Technology, Niigata University, Niigata, Niigata
950-2181, Japan

Abstract. We discuss a method of coincidence analysis to search for gravitational waves from inspiraling compact binaries using the data of two laser interferometer gravitational wave detectors. We examine the allowed difference of the wave's parameters estimated by each detector to obtain good detection efficiency. We also discuss a method to set an upper limit to the event rate from the results of the coincidence analysis. For the purpose to test above methods, we performed a coincidence analysis by applying these methods to the real data of TAMA300 and LISM detectors taken during 2001. We show that the fake event rate is reduced significantly by the coincidence analysis without losing real events very much. Results of the test analysis are also given.

PACS numbers: 95.85.Sz, 04.80.Nn, 07.05.Kf, 95.55.Ym

1. Introduction

Several laser interferometric gravitational wave detectors, such like TAMA300[1], LIGO[2], GEO600[3], and VIRGO[4], have already been constructed or expected to be finished its construction soon.

TAMA300 is an interferometric gravitational wave detector with 300 m baseline length located at Mitaka campus of the National Astronomical Observatory of Japan in Tokyo ($35.68^\circ N, 139.54^\circ E$). LISM is an interferometric gravitational wave detector with 20 m baseline length located at Kamioka mine, Gifu ($36.25^\circ N, 137.18^\circ E$). LISM was originally developed as a prototype detector during 1990 to 1995 in the National Astronomical Observatory in Mitaka, Tokyo. In 2000, it was moved into the Kamioka mine to perform observation.

TAMA300 began to operate in 1999, and performed observations for 7 times by the end of 2002. In particular, during the period from 1 August to 20 September 2001, TAMA300 performed the longest observation, and about 1100 hours of data were

§ E-mail:hirotaka@vega.ess.sci.osaka-u.ac.jp

taken. LISM detector also performed an observation from 1 to 23 August, and 3 to 17 September, 2001, and about 780 hours of data were taken. This observation is called Data Taking 6 (DT6) among the TAMA collaboration and the LISM collaboration. Among the LISM data, the last half of data taken during September are in good condition, and are available for the gravitational wave event searches. As a result, the length of data available for the coincidence analysis is about 275 hours in total. The best sensitivity of the TAMA300 was about $5 \times 10^{-21}/\sqrt{\text{Hz}}$ around 800Hz. The best sensitivity of the LISM was about $6.5 \times 10^{-20}/\sqrt{\text{Hz}}$ around 800Hz.

In the past, only a few works have been done for the coincidence analysis using real data of two or more laser interferometers, although many works has been done using bar detectors. As far as we are aware of, only one coincidence analysis to search for burst events in a pair of laser interferometers has been reported [5]. Although, the sensitivities of TAMA300 and LISM are different for one order of magnitude, it is a very good opportunity to perform coincidence analysis since long data are available, and both detector have shown good stability which allow us to perform such analysis.

We consider gravitational waves from inspiraling compact binaries, consisting of neutron stars or black holes. Since their wave forms are well known by post-Newtonian approximation of general relativity, we can use the matched filtering. In this paper, we discuss a method of coincidence analysis to search for inspiraling compact binaries by using the results of the matched filtering search by several interferometers.

The outline of the analysis discussed here is as follows. We independently performed a matched filtering search in each detector and obtain event lists. We compare the lists to find coincident events. In matched filtering search, each event depends not only on the time of coalescence but also on two masses, and so on. We can thus require consistency conditions for such parameters by which we decide whether each pair of events in the event lists can be considered as a coincident event. By requiring such condition, we can reduce the false alarm rate significantly. It is important to determine the consistency condition so that we do not lose real events very much. We evaluate the errors of estimated parameters by using Fisher matrix and by monte carlo simulations. Those estimate of errors are used in the coincident event search as windows of parameters allowed for each pair of events. In real data analysis, it is important to check the detection efficiency. Thus, we briefly discuss the detection efficiency by using test signals injected into TAMA300 and LISM data.

To test the performance of the above method, we perform the coincidence analysis using short length of data of TAMA300 and LISM. We find that significant number of fake events are removed by coincidence analysis without losing real signals significantly.

After comparing the event lists by requiring consistency conditions, we have a list of candidate events. In order to state any statistical significance of these events, we need to compare the number of survived events with estimated number of coincident events produced accidentally by fake events. We discuss how to estimate the number of events produced accidentally.

Finally, we discuss a method to set an upper limit to the event rate using coincident

event lists. To test the method, this method is applied to the above test results. The results for the upper limit given here can not be considered as our final scientific results, since our objective here is to test the method using the short length of real interferometers' data. Complete results of the analysis using all the data of TAMA300 and LISM during 2001 will be discussed in a separated paper [6].

This paper is organized as follows. In section 2, theoretical wave forms, basic formulas of matched filtering, and χ^2 method to reject non-stationary, non-Gaussian noise events are shown. In section 3, a method of coincidence analysis are proposed, and detection efficiency are evaluated using TAMA300 and LISM data. In section 4, We apply the above method to real data of TAMA300 and LISM, and obtain a coincident event list. Using the list, we evaluate the number of accidental coincident events, and discuss the statistical significance of events. In section 5, we discuss a method to set an upper limit to the Galactic events. Section 6 is devoted to the summary and discussions.

2. Matched filtering

We assume that the time sequential data of the detector output $s(t)$ consists of a signal plus noise $n(t)$. To characterize the detector's noise, we denote the one-sided power spectrum density of noise by $S_n(f)$. We also assume that the wave forms of the signals are predicted theoretically with sufficiently good accuracy. We call these wave forms as *templates*. We adopt templates calculated by using the post-Newtonian approximation of general relativity[7]. We use the restricted post-Newtonian wave forms in which the phase evolution is calculated to 2.5 post-Newtonian order, but the amplitude evolution contains only the lowest Newtonian quadrupole contribution. We also use the stationary phase approximation to calculate the Fourier transformation of the wave forms.

We denote the parameters distinguishing different templates by θ^μ . They consist of the coalescence time t_c , the chirp mass $\mathcal{M}(\equiv M\eta^{3/5})$ ($M = m_1 + m_2$), and non-dimensional reduced mass $\eta(\equiv m_1 m_2 / M^2)$. In this analysis, we did not take into account of the effects of spin angular momentum. The templates corresponding to a given set of θ^μ are represented in Fourier space by two independent templates \tilde{h}_c and \tilde{h}_s as

$$\tilde{h}(f) = \tilde{h}_c(f) \cos \phi_c + \tilde{h}_s(f) \sin \phi_c, \quad (1)$$

where ϕ_c is the phase of wave, and

$$\begin{aligned} \tilde{h}_c(\theta^\mu, f) &= i\tilde{h}_s(\theta^\mu, f) = \mathcal{N} f^{-7/6} e^{i(\psi_\alpha(f) + t_c f)}, \\ &\quad \text{for } 0 < f \leq f_{\max}(\theta^\mu), \\ \tilde{h}_c(\theta^\mu, f) &= \tilde{h}_s(\theta^\mu, f) = 0, \\ &\quad \text{for } f > f_{\max}(\theta^\mu). \end{aligned} \quad (2)$$

Here \mathcal{N} is a normalization constant, and

$$\psi_\alpha(f) = \sum_i \alpha^i(\theta^\mu) \zeta_i(f), \quad (3)$$

with

$$\alpha^1 = \frac{3}{128\eta} (\pi M)^{-5/3},$$

$$\begin{aligned}
\alpha^2 &= \frac{1}{384\eta} \left(\frac{3715}{84} + 55\eta \right) (\pi M)^{-1}, \\
\alpha^3 &= -\frac{3\pi}{8\eta} (\pi M)^{-2/3}, \\
\alpha^4 &= \frac{3}{128\eta} \left(\frac{15293365}{508032} + \frac{27145}{504}\eta + \frac{3085}{72}\eta^2 \right) (\pi M)^{-1/3}, \\
\alpha^5 &= \frac{\pi}{128\eta} \left(\frac{38645}{252} + 5\eta \right), \\
\zeta_1(f) &= f^{-5/3}, \quad \zeta_2(f) = f^{-1}, \quad \zeta_3(f) = f^{-2/3}, \\
\zeta_4(f) &= f^{-1/3}, \quad \zeta_5(f) = \ln f.
\end{aligned} \tag{4}$$

Negative frequency components are given by the reality condition of $h(t)$ as $\tilde{h}(-f) = \tilde{h}^*(f)$ where $*$ means the operation of taking the complex conjugate. The value of f_{\max} is determined by a cut off frequency chosen close to the innermost stable circular orbit frequency, f_c , or the half of the sampling frequency of data, f_s . We adopt smaller one from f_c and f_s as f_{\max} .

We define a filtered output by

$$\rho(t_c, m_1, m_2, \phi_c) \equiv 2 \int_{-\infty}^{\infty} \frac{\tilde{s}(f)\tilde{h}^*(f)}{S_h(f)} df = (s|h). \tag{5}$$

In eq. (5), we can analytically take the maximization over ϕ_c which gives

$$\rho(t_c, m_1, m_2) = \sqrt{(s|h_c)^2 + (s|h_s)^2}. \tag{6}$$

We choose the normalization constant \mathcal{N} of the templates so that it satisfies $(h_c|h_c) = (h_s|h_s) = 1$. We can see that ρ has an expectation value $\sqrt{2}$ in the presence of only Gaussian noise. Thus, the signal-to-noise ratio is given by $SNR = \rho/\sqrt{2}$.

Analyzing the real data of TAMA300, we have found that the noise contained a large amount of non-stationary and non-Gaussian noise [8]. In order to remove the influence of such noise, we introduce a χ^2 test of the time-frequency behavior of the signal [10]. Here, χ^2 is defined as follow. First we divide each template into n mutually independent pieces in the frequency domain, chosen so that the expected contribution to ρ from each frequency band is approximately equal, as

$$\tilde{h}_{c,s}(f) = \tilde{h}_{c,s}^{(1)}(f) + \tilde{h}_{c,s}^{(2)}(f) + \cdots + \tilde{h}_{c,s}^{(n)}(f). \tag{7}$$

We calculate

$$\begin{aligned}
z_{(c,s)}^{(i)} &= (\tilde{s}|\tilde{h}_{c,s}^{(i)}), \\
\bar{z}_{(c,s)}^{(i)} &= \frac{1}{n}(\tilde{s}|\tilde{h}_{c,s}),
\end{aligned} \tag{8}$$

The χ^2 is defined by

$$\chi^2 = n \sum_{i=1}^n \left[(z_{(c)}^{(i)} - \bar{z}_{(c)}^{(i)})^2 + (z_{(s)}^{(i)} - \bar{z}_{(s)}^{(i)})^2 \right]. \tag{9}$$

This quantity must satisfy the χ^2 -statistics with $2n - 2$ degrees of freedom, as long as the data consists of Gaussian noise plus chirp signals. For convenience, we renormalized χ^2 as $\chi^2/(2n - 2)$. In this paper, we chose $n = 16$.

The value of χ^2 is independent to the amplitude of the signal as long as the template and the signal have an identical wave form. However, in reality, since the template and the signal have different value of parameters because of the discrete time step and discrete mass parameters we search, the value of χ^2 becomes larger when the amplitude of signal becomes larger. In such situation, if we reject events simply by the value of χ^2 , we may lose real events with large amplitude. We thus introduce a statistic, $\rho/\sqrt{\chi^2}$, to distinguish between candidate events and noise events. By checking the Galactic event efficiency, we found that the selection by the value of $\rho/\sqrt{\chi^2}$ gives reasonable detection efficiency.

We searched for the mass parameters, $1.0M_\odot \leq m_1, m_2 \leq 2.0M_\odot$, which is a typical mass region of neutron stars. In the mass parameter space, we prepared a mesh. The mesh points define templates used for search. The mesh separation is determined so that the maximum loss of SNR becomes less than 3%. We use a special parametrization of mass parameters which was introduced by Tanaka and Tagoshi[9]. This method simplifies algorithm using geometrical arguments to determine the mesh points. The parameter space defined in our search program turned out to contain about 200 \sim 1000 templates for the TAMA300 data, and about 200 \sim 600 templates for the LISM data. The variation of the number of template is due to the variation of the shape of noise power spectrum. The typical value of the number of template is about 700 for TAMA300, and 400 for LISM.

We perform matched filtering search using TAMA300 and LISM data independently. We obtain ρ and χ^2 as functions of masses and the coalescing time t_c . In each small interval of coalescing time Δt_c , we looked for an event which had the maximum ρ . In the search we report in the following sections, we choose $\Delta t_c = 25\text{msec}$.

3. A coincidence analysis

3.1. Algorithm

Each event in the event list, obtained by the matched filtering search independently performed for two detectors, depends on t_c , M , and η . If they are real events, they should have the same parameters in both event lists. However, we may observe real events with different parameters by the effects of detectors' noise and other effects. Therefore we have to determine the allowed difference of parameters by taking into account of these effects, in order not to lose real events by coincidence analysis.

Time selection: First we discuss the coalescence time t_c . The distance between TAMA300 and LISM is 219.92km. Therefore, the maximum delay of the signal arrival time is $\Delta t_{\text{dis}} = 0.73\text{msec}$. The effect of detectors' noise to the estimated value of t_c can be evaluated by the Fisher information matrix[11]. We denote the 1σ value of error for each detector as $\Delta t_{c\text{TAMA,LISM}}$. We can determine allowed error of t_c due to noise by $\Delta t_{\text{noise}} = \sigma \times \Delta t_c$ where $\Delta t_c \equiv \sqrt{\Delta t_{c\text{TAMA}}^2 + \Delta t_{c\text{LISM}}^2}$.

Finally, we define the allowed difference of t_c as follows. If the parameters

t_c^{TAMA} , t_c^{LISM} of the each pair of events satisfy

$$|t_c^{\text{TAMA}} - t_c^{\text{LISM}}| < \Delta t_{\text{dis}} + \Delta t_{\text{noise}}, \quad (10)$$

the event is recorded as a candidate event.

Note that the Gaussian distribution of the noise and the large amplitude of the events are assumed in evaluating the 1σ error of the estimated parameter due to noise. Thus, in applying the real data analysis in which the noise is not necessary Gaussian, and the amplitude of events are not necessary very large, we have to check the detection efficiency by other methods. As discussed in the next section, we find that if we adopt $\sigma > 3$, we will be able to obtain very high detection probability even in the case of real data.

Mass selection: Next we discuss the mass parameters. The error of estimated parameter of the chirp mass and reduced mass due to noise can also be evaluated by the Fisher matrix. We denote it by $\Delta\mathcal{M}_{\text{noise}}$ and $\Delta\eta_{\text{noise}}$, which are evaluated from each detector as

$$\begin{aligned} \Delta\mathcal{M}_{\text{noise}} &= \sigma \sqrt{\Delta\mathcal{M}_{\text{TAMA}}^2 + \Delta\mathcal{M}_{\text{LISM}}^2}, \\ \Delta\eta_{\text{noise}} &= \sigma \sqrt{\Delta\eta_{\text{TAMA}}^2 + \Delta\eta_{\text{LISM}}^2}, \end{aligned}$$

where $\Delta\mathcal{M}_i$ and $\Delta\eta_i$ are 1σ value of error induced by each detector's noise. The value of σ will be discussed in the next subsection.

Along with the error due to noise, we also have to take into account of the effect of the finite mesh size. When the amplitude of the signal is very large, the errors evaluated by the Fisher matrix becomes smaller than the value of finite mesh size, since the error of the parameter due to noise is inversely proportional to the value of ρ . We denote the error due to the finite mesh size as $\Delta\mathcal{M}_{\text{mesh}}$, $\Delta\eta_{\text{mesh}}$. We determine the allowed difference of the chirp mass and the reduced mass so that if the parameters $\mathcal{M}^{\text{TAMA}}$, $\mathcal{M}^{\text{LISM}}$, η^{TAMA} and η^{LISM} of each pair of events satisfy

$$\begin{aligned} |\mathcal{M}^{\text{TAMA}} - \mathcal{M}^{\text{LISM}}| &< \max(\Delta\mathcal{M}_{\text{noise}}, \Delta\mathcal{M}_{\text{mesh}}), \\ |\eta^{\text{TAMA}} - \eta^{\text{LISM}}| &< \max(\Delta\eta_{\text{noise}}, \Delta\eta_{\text{mesh}}), \end{aligned} \quad (11)$$

the pair of event is adopted as a candidate event.

Amplitude selection: Next we discuss the amplitude. When the sensitivity of the detectors is different, the signal-to-noise ratio observed by each detector will be different. Further, since the direction of the arm of each interferometer will be different in general, the signal-to-noise ratio will be different in each detector even if the sensitivity is the same. Even in such cases, we can still require consistency condition to the events and reduce the number of fake events.

In our case, the sensitivity of TAMA300 is typically 15 times better than that of LISM. We can simply express this effect by δ_{sens} defined as

$$\delta_{\text{sens}} \equiv \log \left[\left(\int \frac{f^{-7/3}}{S_{n \text{ TAMA}}(f)} df \right)^{1/2} / \left(\int \frac{f^{-7/3}}{S_{n \text{ LISM}}(f)} df \right)^{1/2} \right]. \quad (12)$$

The arm direction of LISM is rotated from that of TAMA300 for 60 degrees. Real events will be detected with different SNR by each detector depending on its incident

direction and polarization. A simple and straightforward way to evaluate the allowed difference of amplitude is to perform simulations. To evaluate only the effect of different arm direction, we assume two detectors have identical noise power spectrum. We then perform simulations by generating the Galactic events and by evaluating the difference of ρ which are detected by each detector. We then determine the value of δ_{simu} such that for more than 99.9 % of events, we have

$$-\delta_{\text{simu}} \leq \log \left(\frac{\rho_{\text{TAMA}}}{\rho_{\text{LISM}}} \right) \leq \delta_{\text{simu}}. \quad (13)$$

There is also an error due to noise in the estimated value of ρ which can also be estimated by the Fisher matrix in the same way as t_c , \mathcal{M} and η . We denote it as δ_{noise} .

By combining the above two effects, we determine the allowed difference of ρ_{TAMA} and ρ_{LISM} by

$$\delta_{\text{sens}} - \delta_{\text{simu}} - \delta_{\text{noise}} \leq \log \left(\frac{\rho_{\text{TAMA}}}{\rho_{\text{LISM}}} \right) \leq \delta_{\text{sens}} + \delta_{\text{simu}} + \delta_{\text{noise}}. \quad (14)$$

3.2. Efficiency

Here, we discuss the detection efficiency of the algorithm of the coincidence analysis discussed in the previous subsection. As model sources, we generate inspiraling compact binaries located within 1 kpc from Solar system in our Galaxy. The distribution of the binaries are determined so that it reproduce a density distribution [10]. Other parameters like two masses, the inclination angle, the polarization angle, and phase are determined randomly. We consider the mass from $1M_{\odot}$ to $2M_{\odot}$ for each star. We inject 1000 events into TAMA300 and LISM data, and analyse the data using the algorithm discussed in the previous section. When we set a threshold $\rho > 7$, the detection efficiency of the independent analysis of TAMA300 and LISM becomes 99% and 33% respectively. Since we perform coincidence analysis, the maximum value of the detection efficiency is limited by LISM's efficiency. We thus show the relative efficiency of the analysis, after applying criteria of coincidence, compared to the one detector efficiency of LISM in Fig.1. We find that, among 33 % of events which are detected by LISM, we can detect even after the coincidence analysis more than 94 % if we set $\sigma > 3$. Thus, in the analysis discussed in the next section, we adopt a precise $\sigma = 3.29$ because it corresponds to 0.1% probability of losing real events in Gaussian noise case.

4. Application to TAMA300 and LISM data

4.1. Results of coincidence analysis

We perform a matched filtering search using TAMA300 and LISM data respectively. For the purpose of test analysis, we use 26.0 hours of data for which both detector were locked. This length is about 10% of all the data available for coincidence analysis taken during Data Taking 6. As results of matched filtering search, there are 159,935 events for TAMA300 and 109,609 events for LISM.

For these candidate events, we perform a coincidence analysis by requiring consistency among the parameters. The consistency conditions are imposed in the order of the coalescence time selection, the mass selection and the amplitude selection. In Table 4.1, we show the results of the coincident event search. In Fig.2, we also show a scatter plot of the coincident events after coincidence selections in terms of the value of ρ_{TAMA} and ρ_{LISM} .

Although significant number of fake events are removed by taking coincidence, there still remains many events with large χ^2 . Thus, we can obtain better detection efficiency if we introduce a χ^2 selection in addition to the coincidence selections. In Fig.3, we also show a scatter plot of the coincident events after coincidence selections in terms of the value of $\rho_{\text{TAMA}}/\sqrt{\chi_{\text{TAMA}}^2}$ and $\rho_{\text{LISM}}/\sqrt{\chi_{\text{LISM}}^2}$.

We examine the distribution of ρ and $\sqrt{\chi^2}$ for each detector. The peak value of $\rho_{\text{TAMA}}, \rho_{\text{LISM}}, \sqrt{\chi_{\text{TAMA}}^2}$ and $\sqrt{\chi_{\text{LISM}}^2}$ are 8.90, 10.18, 2.38, 2.80. It is expected from this that the value of $\rho/\sqrt{\chi^2}$ of the coincident events are distributed around $\rho/\sqrt{\chi^2} \sim 4$. In Fig.3, we find that the distribution of the coincident events are consistent with this expectation.

By injecting test signals into data, it is confirmed that when signals with $\rho = 20$ are detected, the value of $\sqrt{\chi^2}$ become $\sqrt{\chi^2} \sim 1.3$, Such events have value $\rho/\sqrt{\chi^2} \sim 15$. Thus, from Fig.3, if such events really happened, the value of $\rho/\sqrt{\chi^2}$ would become much larger than the tail of the distribution of coincident events. For TAMA300, the value $\rho \sim 20$ will be produced by events occurring in the center of the Galaxy, although the distance will be much shorter for LISM.

Table 1. Results of the coincidence analysis. n_{obs} is the number of coincident events. $\bar{n}_{\text{acc}}, \bar{\sigma}_{\text{acc}}$ are the estimated number of accidental coincidence and its standard deviation.

	n_{obs}	$\bar{n}_{\text{acc}} \pm \bar{\sigma}_{\text{acc}}$
after time selection	486	579.13 ± 248.57
after time and mass selection	74	84.68 ± 34.72
after time, mass and amplitude selection	63	67.14 ± 32.90

4.2. Accidental coincidence

In this section we discuss how to estimate the number of accidental coincident events. It is possible to estimate the number of accidental coincident events by a usual procedure of shifting one of two sets of data by a time δt (called time delay) and determining the number of coincidence $n_c(\delta t)$ [12] [13]. Repeating for m different values of time delay, the expected number of coincidence is simply the sample mean of the m values of $n_c(\delta t)$ at delays other than $\delta t = 0$,

$$\bar{n}_{\text{acc}} = \frac{1}{m} \sum_{i=1}^m n_c(\delta t_i). \quad (15)$$

The corresponding experimental standard deviation is given by

$$\bar{\sigma}_{acc} = \sqrt{\sum_{i=1}^m \left(n_c(\delta t_i) - \bar{n}_{acc} \right)^2 / m}. \quad (16)$$

Since there is no signal at delays other than $\delta t = 0$, the number of coincident events at these delays can be considered as an experimental estimation of the parent distribution from which the accidental coincidence are drawn.

In this analysis, we performed the time shift for 400 times between $-40,000$ seconds and $40,000$ seconds. Each time shift is separated with another time shift for 200 seconds.

The number of accidental coincidence and its standard deviation is shown in Table.1. We can see that the number of coincident events obtained after each selection is completely agree with the number of accidental coincidence. Thus, we conclude that we find no signature of gravitational wave events in the data used here.

By examining the event rate of each detector in each 100seconds interval, we find that the events rate are nearly stationary in the period of 26 hours in both detectors, except a few portions which show the event rate $7 \sim 10$ larger than the other normal portions. Since we did not excluded such burst like portions in the time shift procedure, the average and the variance of the number of accidental coincident events are slightly affected by such portions. If we exclude such portions, the average of accidental coincidence becomes smaller, and the value becomes more closely to the observed value. The variance also becomes smaller. However, since the main purpose of the analysis here is to test our coincidence procedure, we do not discuss it furthermore here.

5. Upper limit to the Galactic event rate

In this section, we discuss a method to evaluate the upper limit to the Galactic event rate based on the result of the coincidence analysis. As sources, we consider nearby events within 1kpc from the Solar system in our Galaxy.

The upper limit to the event rate is given by $N/(T\epsilon)$, where N is an upper limit to the average number of real events over a certain threshold, T is length of data [hours] and ϵ is the detection efficiency.

First, we evaluate an upper limit to average number of real events, N , over a threshold. Assuming Poisson distribution for the number of real/fake events over a threshold, we can obtain an upper limit to the expected number of real events, N , as a solution of [14]

$$\frac{e^{-(N+N_{bg})} \sum_{n=0}^{n=N_{OBS}} \frac{(N+N_{bg})^n}{n!}}{e^{-(N_{bg})} \sum_{n=0}^{n=N_{OBS}} \frac{(N_{bg})^n}{n!}} = 1 - \text{C.L.} \quad (17)$$

where N_{obs} is an observed number of events over the threshold and N_{bg} is an estimated number of fake events over the threshold, C.L. is a confidence level.

In order to determined the threshold, in stead of defining the single signal-to-noise ratio, we define thresholds to the value of $\rho_{\text{TAMA}}/\sqrt{\chi_{\text{TAMA}}^2}$ and $\rho_{\text{LISM}}/\sqrt{\chi_{\text{LISM}}^2}$. From

Fig.3, we set a threshold for TAMA300 to $\rho_{\text{TAMA}}/\sqrt{\chi_{\text{TAMA}}^2} = 7.27$, and for LISM to $\rho_{\text{LISM}}/\sqrt{\chi_{\text{LISM}}^2} = 7.47$. Observed number of events over these thresholds is $N_{\text{obs}} = 0$. We can also evaluate expected number of fake events over thresholds to be $N_{\text{bg}} = 0.74$ which corresponds to the false alarm rate, 0.028 events/hours. Using Eq.(17), we obtain upper limit to the average number of real events over the threshold as $N = 2.30$ (C.L. = 90%).

Second, we evaluate detection efficiency ϵ by simulations explained in section 3.2. With the threshold determined above, we obtain the probability that we detect events over the each detector's threshold as $\epsilon = 0.20$.

Using above results and the length of data $T = 26.0$ [hours], we obtain an upper limit to the event rate of near by sources in 1kpc to be $N/(T\epsilon) = 0.44$ events/hour (C.L.= 90%). This value is not improved from the value obtained by the analysis of TAMA300 alone. This is because the sensitivity of TAMA300 is nearly 100 % in this distance, although the sensitivity of LISM is still less than 30 %. In such situation, the gain of efficiency obtained due to lower threshold is dominated by the lower sensitivity of LISM, since the efficiency of coincidence is limited by the detector with lower sensitivity.

6. Summary

In this paper, we discussed a method of the coincidence analysis to search for inspiraling compact binaries using matched filtering. We examined the selection criteria for coincidence of the parameters like the time of coalescence, chirp mass, reduced mass, and the amplitude of events. We found, by simulation using the data of TAMA300 and LISM, that we do not lose events significantly by appropriately choosing the selection criteria. The method discussed in this paper can easily applicable to multiple detectors cases in which more than two detectors are used.

For the test purpose, we performed coincidence analysis using the short length of data of TAMA300 and LISM taken during DT6 observation in 2001. We found that significant number of fake events are removed by taking coincidence.

Since the sensitivity of TAMA300 is much better than LISM, the detection efficiency after coincidence analysis does not improved compared to that of TAMA300 alone, although we can have a better efficiency compared to that of LISM alone. Thus, we do not have an improved upper limit to the event rate compared to the result obtained by TAMA300 alone. However, when two detectors have comparable sensitivity, it is possible to obtain an improved sensitivity compared to the one detector analysis. Further, in any cases, when we find candidate gravitational wave events, its statistical significance becomes larger by taking coincidence.

Complete results of the analysis, including an upper limit to the event rate using all the data of TAMA300 and LISM during Data Taking 6 will be reported elsewhere [6].

This work was supported in part by Grant-in-Aid for Scientific Research, Nos. 14047214 and 12640269, of the Ministry of Education, Culture, Sports, Science, and Technology of Japan.

References

- [1] K. Tsubono, in *Gravitational Wave Experiments*, edited by E. Coccia, G. Pizzella, and F. Ronga, (World Scientific, Singapore, 1995).
- [2] A. Abramovici et al., *Science* **256**, 325 (1992).
- [3] K. Danzmann et al., in *Gravitational Wave Experiments*, edited by E. Coccia, G. Pizzella, and F. Ronga, (World Scientific, Singapore, 1995).
- [4] B. Caron et al., in *Gravitational Wave Experiments*, edited by E. Coccia, G. Pizzella, and F. Ronga, (World Scientific, Singapore, 1995).
- [5] D. Nicholson et al., *Phys. Lett. A*, **218**, 175 (1996).
- [6] H. Takahashi et al., in preparation.
- [7] L. Blanchet et al., *Phys. Rev. Lett.* **74**, 3515 (1995).
- [8] H. Tagoshi et al., *Phys. Rev.* **D63**, 062001 (2001).
- [9] T. Tanaka and H. Tagoshi, *Phys. Rev.* **D62**, 082001 (2000).
- [10] B. Allen et al., *Phys. Rev. Lett.* **62**, 1489 (1999).
- [11] C. Cutler and É. E. Flanagan, *Phys. Rev.* **D49**, 082001 (1994).
- [12] E. Amaldi et al., *Astron. Astrophys.* **216**, 325 (1989).
- [13] P. Astone et al., *Phys. Rev.* **D59**, 122001 (1999).
- [14] For example, Particle Data Group, *Review of particle Physics*, *Phys. Letts.* **B204**, 81 (1988).

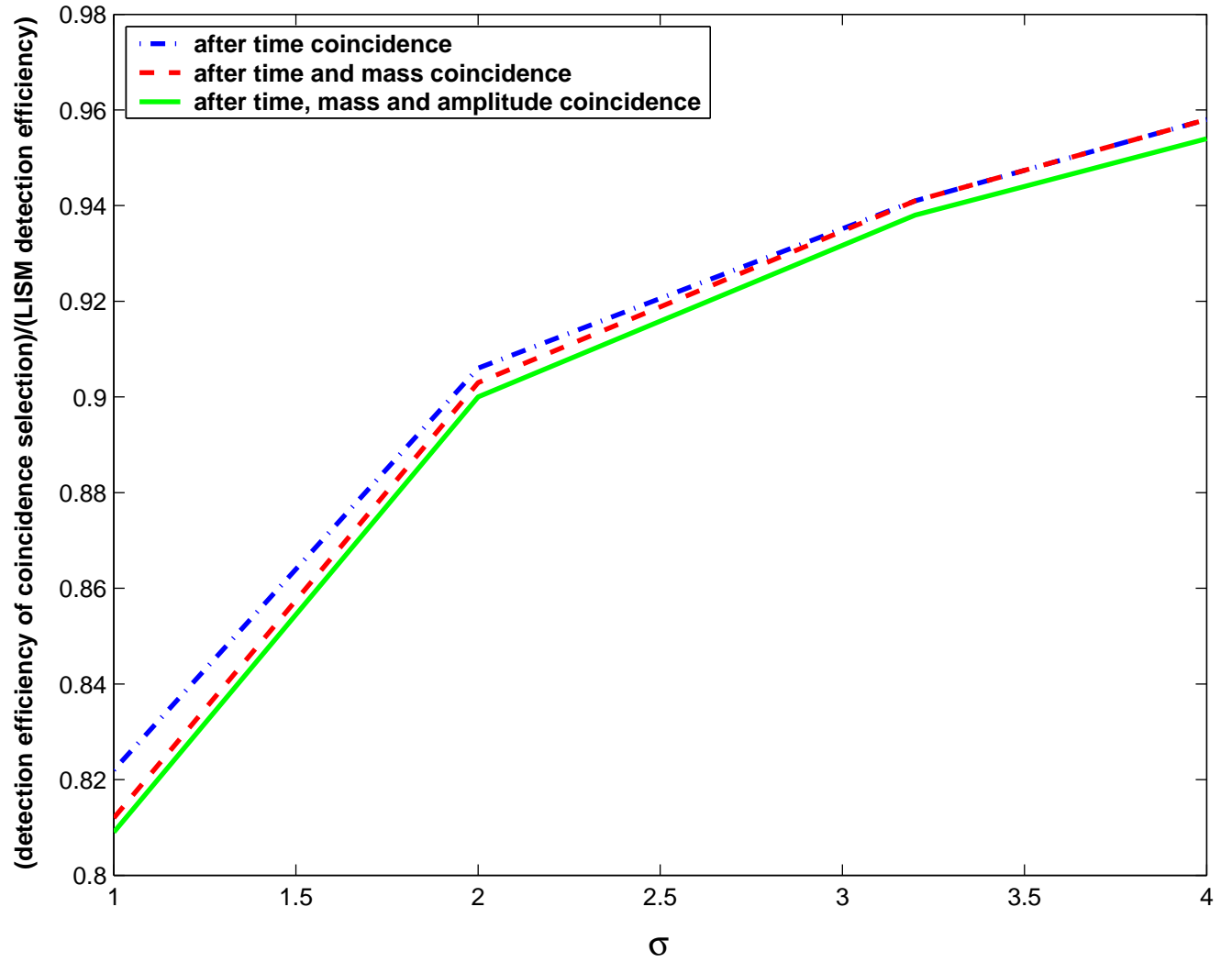


Figure 1. Relative detection efficiency of the coincidence analysis compared to the one detector efficiency of LISM, as a function of a parameter of coincidence selection σ . Dot-dashed line is the efficiency after the time selection, dashed line is the efficiency after the time and mass selection, and solid line is the efficiency after the time - mass - amplitude selection.

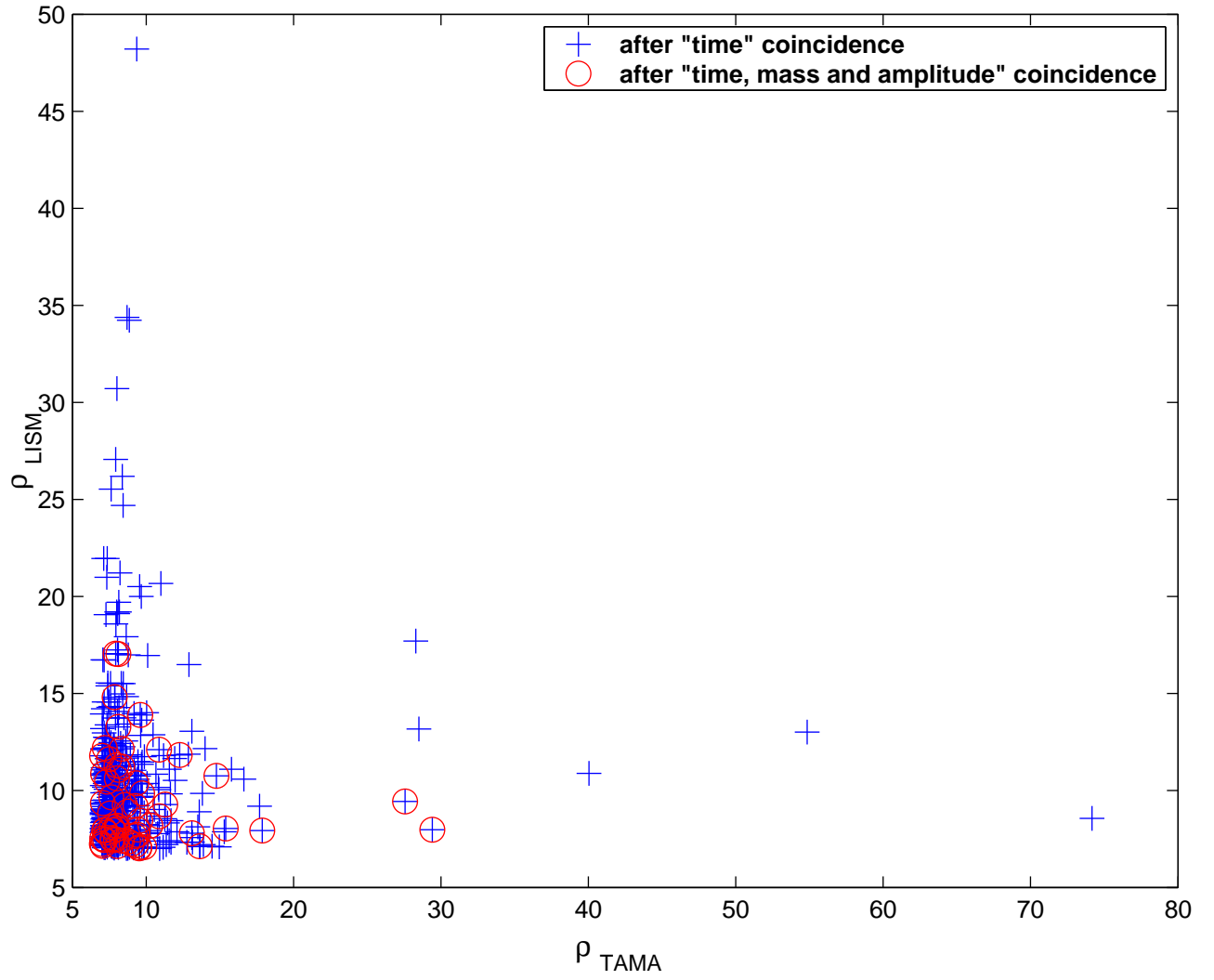


Figure 2. ρ_{TAMA} - ρ_{LISM} scatter plots. The + marks represent the events survived time selection, and circle marks represent the events survived the time, mass and amplitude selection.

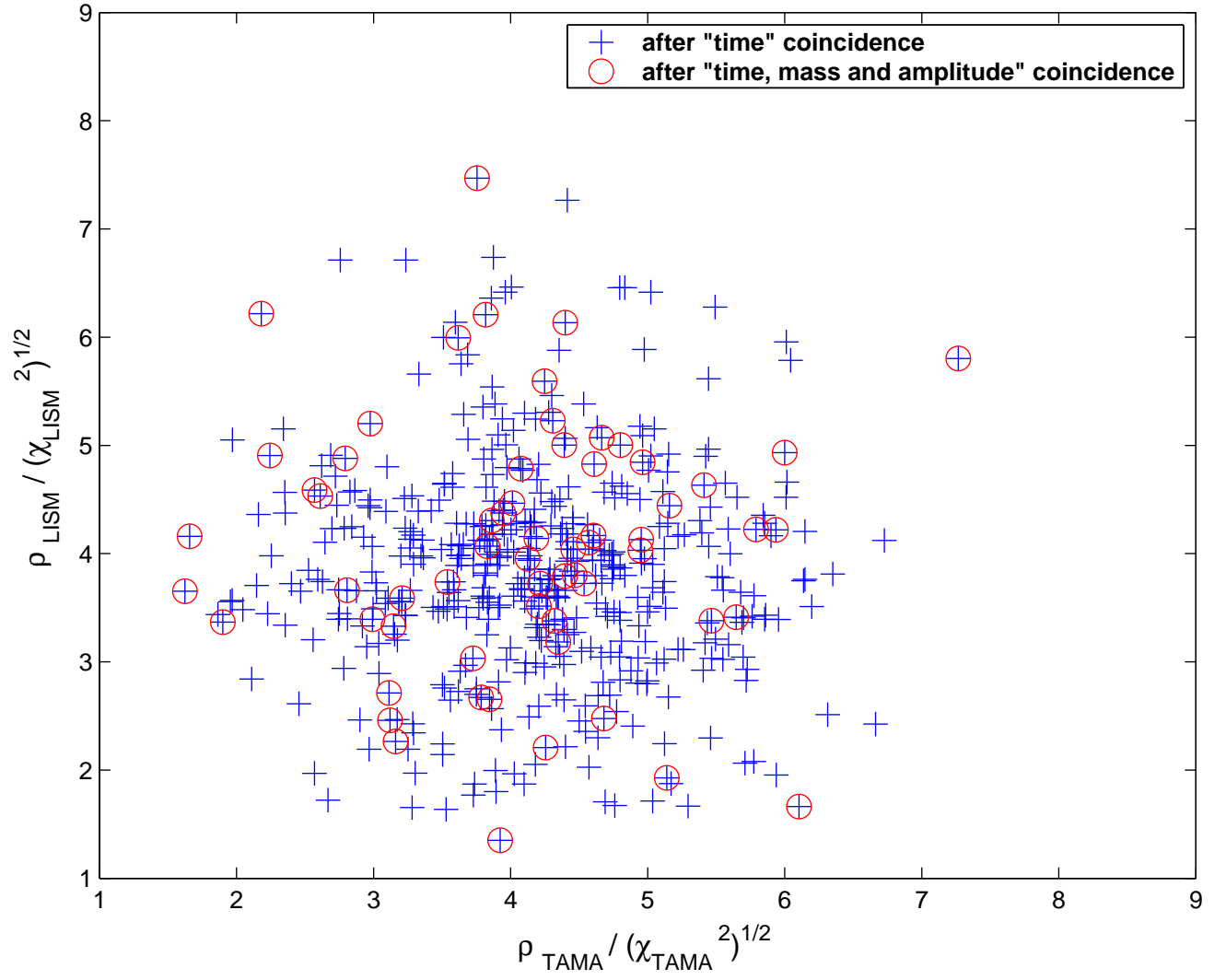


Figure 3. $\rho_{\text{TAMA}} / \sqrt{\chi_{\text{TAMA}}^2} - \rho_{\text{LISM}} / \sqrt{\chi_{\text{LISM}}^2}$ scatter plots. The + marks represent the events survived the time selection and circle marks represent the events survived the time, mass and amplitude selection.